Article ID:1004-4213(2010)10-1889-7

Elimination of Atmospheric Interfering Absorption for the Measurement of Glyoxal by LP-DOAS*

PENG Fu-min[1,3], LUO Tao[2,†], YUAN Yu-peng[1], QIU Ling-guang[1], XIE Pin-hua[3], LIU Wen-qing[3]

(1 *Laboratory of Advanced Porous Materials and College of Chemistry and Chemical Engineering, Anhui University, Hefei* 230039, *China*)

(2 *Key Laboratory of Biomimetic Sensing and Advanced Robot Technology, Hefei Institute of Intelligent Machines, Chinese Academy of Sciences, Hefei*, 230031, *China*)

(3 *Anhui Institute of Optics & Fine Mechanics, Chinese Academy of Sciences, Hefei* 230031, *China*)

Abstract: When measuring glyoxal directly in the atmosphere by Long Path Differential Optical Absorption Spectroscopy (LP-DOAS), the analysis of glyoxal strongly suffers from the cross interference of other absorbers or structure (Xe lamp-structure, H_2O, O_4 and NO_2 absorption). The retrieval method of glyoxal-the elimination of interfering absorption or structure was studied. The Xe lamp-structure will change nonlinearly resulted from the change of pressure broadening and Doppler Broadening with the change of of Xe lamp pressure or temperature. The different lamp reference spectra detected at different time were interpolated to eliminate lamp structure and the resulting residual structures caused by an incorrect elimination were a factor of three below the detection limit of glyoxal; high amount of H_2O in the atmosphere cause the nonlinear absorption of H_2O and the observed band shape to vary with the column density of H_2O. Two H_2O absorption spectra with higher and lower column density were interpolated to eliminate nonlinear H_2O absorption and the resulting residual structures caused by an incorrect elimination were ten times below the detection limit of glyoxal. In addition, the strong absorption of interfering species NO_2 and O_4 were also accurately removed. Low detection limit (0.15 ppbv) and low systematic errors (~10 %) were achieved by the accurate elimination of interfering structures. In the end, glyoxal was routinely detected during the daytime on the outskirts of Guangzhou, where mixing ratios ranged from less than detection limit (0.15 ppbv) to 1.66 ppbv. The variation and range of glyoxal concentration detected agreed well with the results reported.

Key words: Long Path Differential Optical Absorption Spectroscopy (LP-DOAS); Glyoxal; Volatile organic compounds (VOCs); Spectral interpolation

CLCN:O433h **Document Code**:A **doi**:10.3788/gzxb20103910.1889

0 Introduction

In the past, the crucial role of volatile organic compounds (VOCs) has been well established in the formation of photochemical smog[1-2]. It not only poses threat to ambient air quality, but also causes adverse effects on human health[3], agriculture[4], and regional climate[5]. The development of robust control strategies to reduce O_3 and aerosol levels in urban air requires the identification and measurement of molecules that indicate the rate of VOCs oxidation. In urban air, effectors to use indicators to monitor the rate of VOCs oxidation are an effective technique. Glyoxal (CHOCHO), as a new useful indictor for VOCs chemistry, is recognized recently[6]. It′s the smallest α-dicarbonyl and a mutagenic product formed from the oxidation of numerous VOCs[7]; minor amounts have been reported in biogenic and anthropogenic emissions[8-9]. During the day, photolysis and reaction with OH-radicals determine its atmospheric residence time[10]. Fewer atmospheric measurements of glyoxal were carried

*Supported by the National Natural Science Foundation of China (10979014、60801021、51002001 and 20971001), the National Basic Research Program of China (2007CB613305), Anhui Provincial Natural Science Foundation (090414164), Anhui Key Laboratory of Controllable Chemistry Reaction & Material Chemical Engineering (OFCC0901) and the Program for New Century Excellent Talents in University, Ministry of Education (NCET-08-0617)

† Tel:0551-5108212 Email:pengfm79@gmail.com

Received date:2010-07-15 Revised date:2010-09-22

out in the past[6], and LP-DOAS showed great advantages of tracing the variation of this trace gas directly in the atmosphere directly. Here the measurement method and data retrieval method of glyoxal were studied in detail. In addition, the major error-the fitting error was decreased greatly by using interpolation to eliminate lamp structure and H_2O absorption features and the resulting residual structures caused by an incorrect elimination were a factor of three and ten below the detection limit of glyoxal, respectively. The source of systematic error of the glyoxal concentrations determined by the DOAS technique was discussed. With low detection limit (0.15 ppbv), high linearity and low measurement errors (~10%), glyoxal proved to be accurately determined by the used measurement method and retrieval methods.

1 Theories

DOAS technique is based on the optical absorption of gases to determine concentrations of gases using Beer-Lambert law[11-14], Further details are described elsewhere[11-13].

2 Measurement algorithms

2.1 Location

The concentration of glyoxal was monitored using a LP-DOAS instrument on the west outskirts of Guangzhou (China) during summer 2006. DOAS setup was deployed on the third floor and an array of retro-reflectors placed on another building 1.53 km away and 10 m above the ground on the average.

2.2 Measurement system

DOAS system: a Cassegrain telescope with a high pressure Xenon short-arc lamp as the light source; a band pass filter was used. The spectrometer (λ_{blaze} = 500 nm, 600 grooves · mm^{-1}, 0.42 nm spectral resolution, 100 μm wide entrance slit,) was kept at −40 °C to reduce the effect of thermal noise. The light was detected by 1024 element CCD (Charge Coupled Device). The analog-to-digital converter (ADC) was used to acquire the CCD detector signal. After being processed by ADC, the signal was transferred to the computer. The integration time of the measurement spectra was adjusted automatically to the incoming light intensity, so the glyoxal could be retrieved every 2~15 mins from evaluating the spectral range between 420 and 458 nm.

3 Evalvalution of glyoxal

3.1 Reference spectra

LP-DOAS was used to detect glyoxal by its unique specific narrow-band (< 5 nm) absorption structures in the visible spectral range, that enable DOAS[12] to separate trace gas absorptions from broadband molecule and aerosol extinction in the open atmosphere. The absorption cross section of glyoxal showed strong features in the region of 420 to 458 nm. The recording of reference spectra in the field was not straightforward, because glyoxal in a portable cuvette degraded upon exposure to measurement light, sunlight and the formation of polymers, and could induce spectral interferences from the formation of formaldehyde. In this work, the cross section of glyoxal with high resolution was used[15].

The σ of glyoxal was shown in Fig. 1 with a spectral resolution of 0.42 nm (FWHM: Full Width at Half Maximum)[15]. Glyoxal was inherently calibrated from knowledge of its differential absorption cross-section, which for the three covered lines were 5.3, 2.9 and 2.2×10^{-19} cm^2 at 455, 440, and 428 nm, respectively.

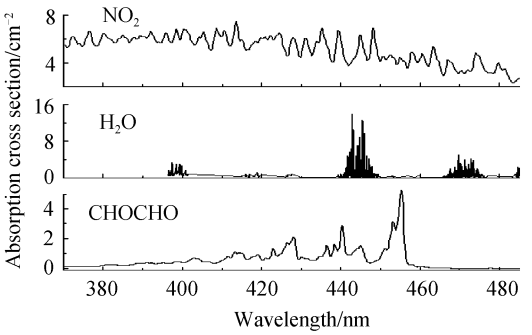

Fig. 1 Absorption cross-section spectra of NO_2, H_2O and glyoxal

3.2 The removing of the interfering absorption

Besides glyoxal, water vapor, NO_2 and O_4 had differential absorption structures in the investigated spectral region (420~458 nm)[6]. In addition, Xenon emission lines (corresponding to an optical density $D=-15\%$ and $D=-8\%$ respectively) from the high pressure arc lamp strongly interfered with the glyoxal absorption structure at 445.1 and 447.3 nm. And it's found that the effect of lamp peaks could not be removed completely by dividing the air spectrum with a measured lamp signal and by high-pass filtering (shown in Fig. 4(a)), because a part of lamp signal emitted to the air was measured as the lamp signal. The lamp signal, therefore, should be

incorporated in a fitting routine as a reference spectrum. The optical density of Xe-structure was so high that the slight changes of it could affect the residual greatly. Shown in Fig. 2, (a) Three lamp spectra (trace A: 07. 23. 2006 08 : 12, trace B: 07. 23. 2006 13 : 52, trace C: 07. 23. 2006 20 : 19). (b) The residual structures after fitting A to B (trace D), C to B (trace F) and A and C (simultaneously) to B (trace E) corresponding to optical density of 0. 29%, 0. 18%, and 0. 019%, respectively. When one lamp reference spectra was used in the fitting process, the lamp structure couldn't be removed completely, and the using of two lamp reference spectra could make the resulting residual structures caused by an incorrect elimination of the water vapor absorption a factor of 3 less than the detection limit of glyoxal.

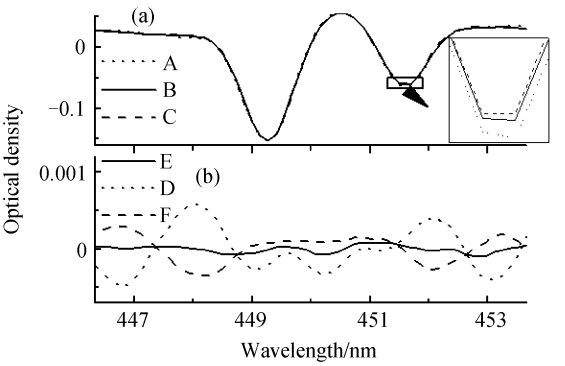

Fig. 2 Lamp structure analysis by LP-DOAS in Guangzhou (2006)

Water vapor had absorption features in this spectral region and at the low resolution of our spectrograph (0. 42 nm), a combination of very strong absorption lines appeared as weak absorption bands in the spectra (Fig. 3). In Fig. 3, (a) Water vapor absorption lines (trace A). (b) Calculated optical densities of water vapor absorption using the low resolution of the spectrograph (0. 42 nm) and water vapor mixing ratios of 0. 021 (trace B), 0. 024 (trace C) and 0. 026 (trace D); (c) The residual structures after fitting B to C (trace F), D to C (trace E) and B and D (simultaneously) to C (trace G) corresponding to optical density of 0. 09%, 0. 08%, and 0. 009%, respectively. During this measurement, water vapor mixing ratios of 2. 1% to 2. 6% were measured resulting in optical densities near 445 nm of the order of 0. 4%～0. 6% (L = 3. 06 km) at our resolution. At these high water vapor column densities (defined as $S = \int_0^L [H_2O]ds$, where L is the length of the light path) of the order of 2.14×10^{23} cm^{-2}, the individual H_2O line had optical densities in excess than 2. 5%.

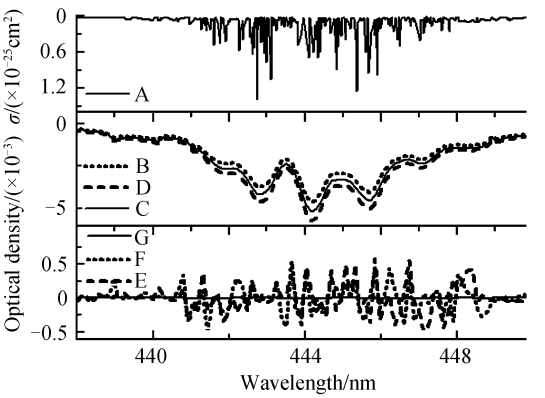

Fig. 3 Simulation of the amount dependence of the water vapor absorption

Due to the convolution with the instrument function the optical density of H_2O was no longer linearly dependent on S. Considering the variation of the water vapor column amount during the measurement, the effects of this non-linear dependence of H_2O absorption bands on the results of the glyoxal were investigated. Different optical densities of water vapor were simulated by applying Lambert-beer's law to the high resolution water absorption cross section[16] and then smoothing the calculated spectrum to simulate the instrumental resolution. Shown in the Fig. 3, it could be seen that the column amount dependent absorption structure of H_2O could be interpolated by simultaneously fitting two water reference spectra, which enclose the optical density of the atmospheric spectrum. The resulting residual structures caused by an incorrect elimination of the water vapor absorption were a factor of ten below the detection limit of glyoxal. Changes of the water vapor absorption structure due to variations of temperature and pressure could be significantly reduced and therefore neglected by the selection of the water vapor reference spectra and the parameters of the numerical filters and the fitting area: the glyoxal data evaluation was restricted to the wavelength intervals 420～458 nm (shown in the Fig. 4). Since glyoxal usually existed at detectable concentrations by day[6], nighttime spectra (at solar zenith angles <80℃) could serve as reference spectra for water absorption[18].

3.3 Spectral fitting process

Firstly, electronic offset and background light were corrected for the measured atmospheric spectra[19]. The air spectrum obtained was divided by the lamp spectrum, high pass filtered and low pass filtered. The reference spectra were prepared by convoluting high resolution absorption spectra

taken from the previous publications with the instrument function[19]. The reference spectra (two H_2O, glyoxal, O_4, NO_2 and two lamps) were subject to the same filtering technique and fitted to the measured spectrum simultaneously[15-19].

Fig. 4 provided an example of the glyoxal evaluation of the DOAS-data from Guangzhou at 10∶11 on 21 July 2006. In the figures, (a) is the measured atmospheric spectrum (A) and scaled lamp reference spectra of B and C (black line); (b) is the residual (D) and scaled water vapor reference spectra E and F; (c) is the residual (G) and scaled reference spectra of NO_2 (H) and O_4 (I); (d) is the residual (J) and scaled reference spectrum of glyoxal (K, 1.21 ppbv); (e) is the residual (here: 1.0×10^{-3} peak to peak). It showed the two lamp reference spectra used to remove lamp structure from the atmospheric spectrum and the elimination of NO_2 and O_4 absorption features. The residual structure after removing H_2O absorption from the spectrum clearly indicated the spectral signature of glyoxal with a concentration of 1.21 ppbv. In the lower most Fig. 4(e), it showed the residual structure remained after subtracting all the reference spectra.

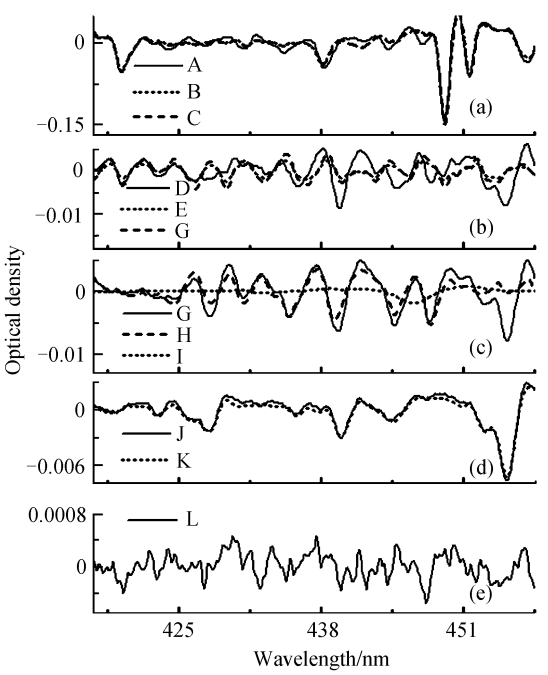

Fig. 4 Sample evaluation of a spectrum measured at 10∶11 am on 21 July 2006

3.4 Measurement results

Glyoxal was detected on all days by DOAS averaging over a 3.06 km optical path on the west outskirts of Guangzhou from 19 to 29 July 2006 except 22 July. The diurnal variation of glyoxal concentration shown in Fig. 5 and Fig. 6 presented the time series of glyoxal concentration. During this time, the highest optical density of glyoxal absorption was 5.1×10^{-3}, corresponding to a concentration of 4.15×10^{10} molec/cm^3 or 1.66 ppbv. The value and the time of glyoxal peak concentrations varied from day to day, and were affected severely by solar radiation. From 20 to 23 July, it's sunny and the concentrations of glyoxal were relatively high; while during the following days, it's cloudy resulting in low concentration of it. Generally, concentrations increased steeply about 1 hour after sunrise (8 A. M.); peaked before and after solar noon (1: 45 P. M.); remained detectable for most of the day; and typically dropped to levels close to the detection limit few hours after sunset (Fig. 6). Virtually no glyoxal was detected during most nights, and concentrations were below the detection limit during early morning hours. Glyoxal peak concentration varied greatly from 1.66 ppbv on sunny day to 0.46 ppbv on cloudy day. The rapid increase of glyoxal shortly after sunrise revealed a very efficient VOCs oxidation process during morning hours (Fig. 6).

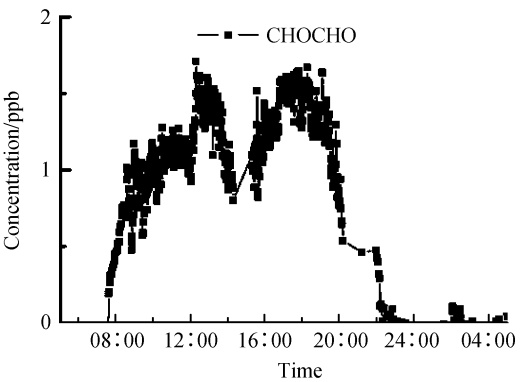

Fig. 5 Concentration time profile of glyoxal measured on 21 July 2006

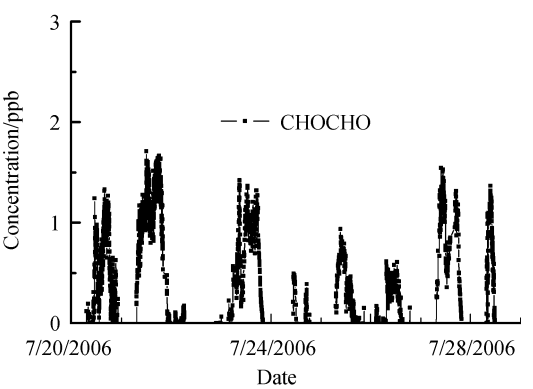

Fig. 6 Time series of glyoxal. Tick marks indicated the beginning of a day

4 Accuracy of concentrations retrieval

4.1 Detection limit

The detection limit of gaseous species depended on the stability of light source, on the intensity of light that reached the spectrograph, on the integration time, on the path length of the DOAS and on the noise of the light detection system. For glyoxal, detection limits were calculated by Eq. (2) [20]

$$C_{\min} = \frac{\tau_{\mathrm{Res}}}{\delta_{(\sigma)} \cdot L} \quad (1)$$

$C_{\min}$ is the smallest concentration of glyoxal, which can be attained by DOAS system; $\delta_{(\sigma)}$ is 1 ppbv glyoxal differential cross section; L is optical path length; τ_{Res} is differential optical density of residual structure, which includes the effects of water vapor, lamp structures and stray light et al. Glyoxal detection limit was 150 ppt in this work.

4.2 Linearity

The linearity of the CCD response was tested between 420 and 458 nm by using different exposure times with light source fixed. The linearity was high enough for the practical use.

In addition, five different amounts of NO_2 standard gases were used to test the linearity of the whole system. Shown in Table 1, the product of the concentration of NO_2 in the cell and the cell length was equal to the product of typical levels of NO_2 in the atmosphere and the practical optical

Table 1 The NO_2 standard gases

	$C_{NO_2} \times L_{cell}$	$C'_{NO_2} \times L_{optical}$
1	250 ppmv × 1.0 1cm	0.82 ppbv × 3.06 km
2	250 ppmv × 15.05 cm	12.25 ppbv × 3.06 km
3	2000 ppmv × 7.99 cm	52.29 ppbv × 3.06 km
4	2000 ppmv × 15.05 cm	98.04 ppbv × 3.06 km
5	2000 ppmv × 50.11 cm	326.80 ppbv × 3.06 km

C_{NO_2}: the concentrations of standard gases; L_{cell}: the length of gas cells; C'_{NO_2}: the theoretical concentrations of gases detected in the practical optical length; $L_{optical}$: the practical optical length.

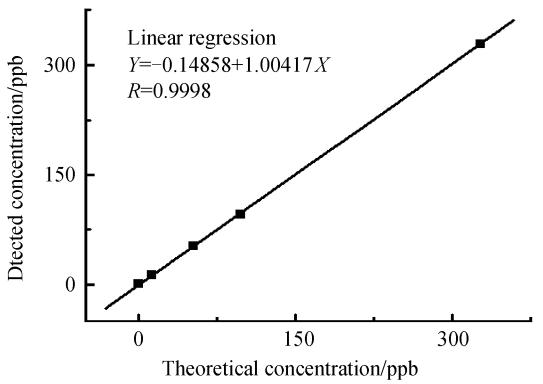

Fig. 7 The linearity of NO_2 response

length of 3.06 km. The linear regression coefficients of $R = 0.999\,8$ was obtained for NO_2 shown in Fig. 7.

4.3 Uncertainties

The uncertainties of glyoxal concentration obtained by DOAS system came from the experiment, the reference cross section of glyoxal and the least squares fitting procedure. During the experiment, offset, dark current and small shift in the spectral dispersion due to temperature changes all could cause some errors. The effect of dark current could be greatly reduced by keeping the CCD at a low temperature (−40℃). Offset was relatively stable and linear to the number of scan, so it could be corrected accurately. The narrow spectral lines of Hg lamp collimated beam from the Cassegrain telescope were used to evaluate the association of a given pixel to the absolute wavelength value, and it was exploited periodically to check and to reset the reference pixel position of the Hg spectral line. In addition, in order to minimize thermal maladjustments, the whole spectrograph unit was thermally isolated and thermo-stated to (30±0.2)℃ by PID controller. Experimental error was estimated below 3% by detecting standard gases of NO_2.

The length of the atmospheric light path was determined with an uncertainty of <1%. In this work the error of cross section used for the glyoxal evaluation was about 5%[15]. The root mean square of the residual (about 8%) was taken as an appropriate estimate of fitting error. So, the whole errors were calculated by Gauss error transfer expressions, the errors of glyoxal in this measurement was therefore <9.9%.

5 Conclusion

In this paper LP-DOAS was developed to measure glyoxal directly in the atmosphere. The retrieval method of glyoxal in the atmosphere was discussed in detail: interpolation was used to eliminate lamp structure and H_2O absorption features and the resulting residual structures caused by an incorrect elimination were a factor of three and ten below the detection limit of glyoxal, respectively; In addition, the strong absorption of interfering species NO_2 and O_4 were also accurately removed. Measurements of glyoxal by DOAS were feasible on a routine basis on the outskirts of Guangzhou. Glyoxal production rates were comparable during morning hours and overhead sun conditions. DOAS can be a powerful tool to

trace concentration variation of this trace gas, with low detection limit (0.15 ppbv), high linearity and low systematic errors (< 9.9 %). Time resolved DOAS measurement of glyoxal places a lower limit on the rate of VOCs oxidation, and provides a novel means to test predictions of smog formation by photochemical models.

References

[1] WANG X S, LI J L, ZHANG Y H, *et al*. Ozone source attribution during a severe photochemical smog episode in Beijing, China[J]. *Science in China Series B Chemistry*, 2009, **52**(8): 1270-1280.

[2] LELIEVELD J, HOOR P, JOCKEL P, *et al*. Severe ozone air pollution in the Persian gulf region[J]. *Atmos Chem Phys*, 2009, **9**(4): 1393-1406.

[3] BERNARD S M, SAMET J M, GRAMBSCH A, *et al*. The potential impacts of climate variability and change on air pollution-related health effects in the United States[J]. *Environmental Health Perspectives*, 2001, **109**(Supp12): 199-209.

[4] GREGG J W, JONES C G, DAWSON T E. Urbanization effects on tree growth in the vicinity of New York City[J]. *Nature*, 2003, **424**(6945): 183-187.

[5] RAMANATHAN V, CRUTZEN P J, KIEHL J T, *et al*. Aerosols, climate, and the hydrological cycle[J]. *Science*, 2001, **294**(5549): 2119-2124.

[6] VOLKAMER R, MOLINA L T, MOLINA M J. DOAS measurement of glyoxal as an indicator for fast VOC chemistry in urban air[J]. *Geophysical Research Letters*, 2005, **32**(L08806): doi: 10.1029/2005GL022616.

[7] VOLKAMER R, PLATT U, WIRTZ K. Primary and secondary glyoxal formation from aromatics: Experimental evidence for the bicycloalkylradical pathway from benzene, toluene, and p-xylene[J]. *J Phys Chem A*, 2001, **105**(38): 7865- 7874.

[8] GROSJEAN D, GROSJEAN E, GERTLER A W. On-road emissions of carbonyls from light-duty and heavy-duty vehicles [J]. *Environ Sci Technol*, 2001, **35**(1): 45- 53.

[9] KEAN A J, GROSJEAN E, GROSJEAN D, *et al*. On-road measurement of carbonyls in California light-duty vehicle emissions[J]. *Environ Sci Technol*, 2001, **35**(21): 4198-4204.

[10] ATKINSON R. Atmospheric chemistry of VOCs and NOx [J]. *Atmos Environ*, 2000, **34**(12-14): 2063-2101.

[11] LIU Cheng, MING Hai, WANG Pei, *et al*. Measurements of the aerosol over naqu of tibet and suburb of beijing by micro pulse lidar (MPL)[J]. *Acta Photonica Sinica*, 2006, **35**(9): 1435-1439.

[12] LIAN Yue, LIU Wen-qing, ZHANG Tian-shu, *et al*. Measurement analysis of atmospheric aerosol aerodynamics size with APD detector[J]. *Acta Photonica Sinica*, 2005, **34**(12): 1837-1840.

[13] FU Qiang, PENG Fu-min, LIU Wen-qing, *et al*. The effect of spectral range on the measurement of ozone in the atmosphere by DOAS[J]. *Spectroscopy and Spectral Analysis*, 2009, **29**(8): 2126-2130.

[14] XIE P, LIU W, SI F, *et al*. Intercomparison of NOx, SO_2, O_3 and aromatic hydrocarbons measured by a commercial DOAS system and traditional point monitoring techniques [J]. *Advances in Atmospheric Sciences*, 2004, **21**(2): 211-219.

[15] VOLKAMER R, SPIETZ P, BURROWS J, *et al*. High-resolution absorption cross-section of glyoxal in the UV - vis and IR spectral ranges[J]. *J Photochem Photobio A: Chem*, 2005, **172**(1): 35-46.

[16] FALLY S. Water vapor line broadening and shifting by air in the 26, 000-13, 000 cm-1 region[J]. *J Quant Spectrosc Radiat Transfer*, 2003, **82**(1-4): 119-131.

[17] ALIWELL S R, JONES R L. Measurement of atmospheric NO_3, 1, Improved removal of water vapor absorption features in the analysis for NO_3[J]. *Geophys Res Lett*, 1996, **23**(19): 2585-2588.

[18] GEYER A, ALICKE B, MIHELCIC D, *et al*. Comparison of tropospheric NO_3 radical measurements by differential optical absorption spectroscopy and matrix isolation electron spin resonance[J]. *J Geophys Res*, 1999, **104**(D21): 26097-26105.

[19] ALICKE B, PLATT U, STUTZ J. Impact of nitrous acid photolysis on the total hydroxyl radical budget during the limitation of oxidant production/pianura padana produzione di ozono study in milan[J]. *J Geophys Res*, 2002, **107**(D22): 8196.

[20] PENG Fu-min, XIE Pin-hua, LIN Yi-hui. Detection of atmospheric NO_2, SO_2 and O_3 using DOAS with a miniaturized fibre-optic spectroscopy system [J]. *Acta Photonica Sinica*, 2008, **37**(11): 2191-2197.

LP-DOAS 测量乙二醛时大气中干扰吸收的去除

彭夫敏[1,3],罗涛[2],袁玉鹏[1],裘灵光[1],谢品华[3],刘文清[3]
(1 安徽大学 化学化工学院 先进多孔材料实验室,合肥 230039)
(2 中国科学院智能机械研究所 仿生传感与先进机器人重点实验室, 合肥 230031)
(3 中国科学院合肥物质科学研究院,合肥 230031)

摘 要:针对利用长光程差分吸收光谱技术在实现对大气中乙二醛实时监测中,一些干扰结构(Xe 灯结构,H_2O、NO_2 和 O_4 干扰吸收)对长光程差分吸收光谱技术的影响,讨论了乙二醛的光谱反演方法对干扰吸收的准确去除.针对 Xe 灯结构由于压力和多普勒展宽程度等的变化而引起的 Xe 灯结构的非线性变化,采用不同时刻的参考灯谱通过光谱插值的方式准确去除,其去除误差引起的剩余结构可降低到比乙二醛的最低理论检测限低 3 倍;针对 H_2O 的非线性吸收以及特征吸收结构随柱浓度的不同而变化的特点,采用较高和较低浓度 H_2O 吸收光谱插值的方法准确去除了严重干扰乙二醛准确反演的 H_2O 的吸收结构,其去除误差引起的剩余结构可降低到比乙二醛的最低理论检测限低 10 倍;另外,对于在此波段存在干扰的 NO_2 和 O_4 的吸收结构也实现了准确地去除.干扰结构的准确去除使 DOAS 对乙二醛的监测实现了较低的实际检测限(0.15 ppbv)和较低的测量误差 (~10 %).最后,在广州郊区对实际大气进行了实际监测,其浓度范围在低于检测限到 1.66 ppbv 之间,与文献报道的浓度范围和变化趋势十分吻合.

关键词:长光程差分吸收光谱;乙二醛;挥发性有机物;光谱插值

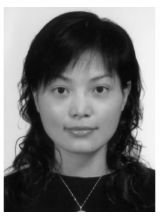

PENG Fu-min was born in 1979. She received the Ph. D. degree from Anhui Institute of Optical and Fine Mechanics, CAS in 2007. Now she is an associate professor of Anhui University.